Journal of Power Sources 578 (2023) 233242

Contents lists available at ScienceDirect

Journal of Power Sources

journal homepage: www.elsevier.com/locate/jpowsour

An ex-situ investigation of the effect of clamping pressure on the membrane swelling of a polymer electrolyte water electrolyzer using X-Ray tomography

Eugen Hoppe [a,*], Sebastian Holtwerth [a,b], Martin Müller [a], Werner Lehnert [a,b]

[a] Forschungszentrum Jülich GmbH, Institute of Energy and Climate Research, IEK-14: Electrochemical Process Engineering, 52425 Jülich, Germany
[b] RWTH Aachen University, Modeling in Electrochemical Process Engineering, 52062 Aachen, Germany

GRAPHICAL ABSTRACT

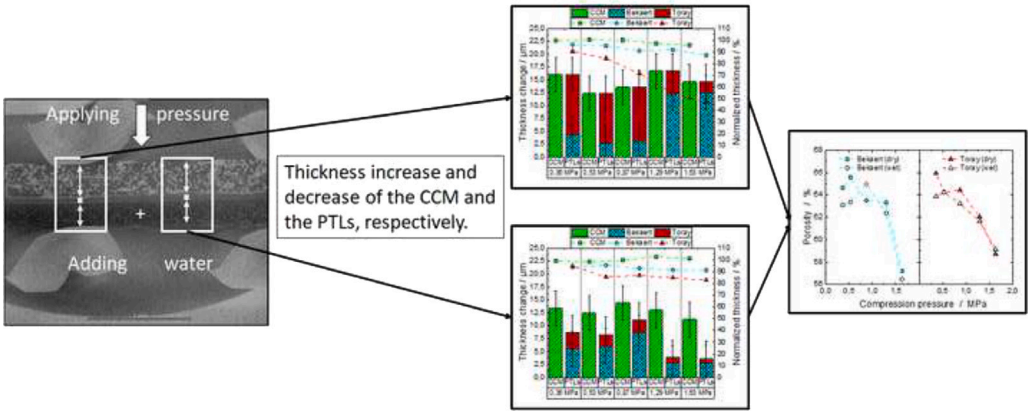

HIGHLIGHTS

- Visualization of membrane-swelling
- Increasing the clamping pressure locally reduces the water uptake of a Nafion® 212 membrane
- Membrane swelling reduces the porosity of the PTL by one percentage-point.

ARTICLE INFO

Keywords:
CCM swelling
X-Ray tomography
PEM water electrolysis

ABSTRACT

Due to water uptake, the polymer membrane of polymer electrolyte membrane water electrolyzers (PEMWE) swells, increases in thickness and so induces swelling pressure. The water content in the membrane and catalyst coated membrane (CCM), respectively, defines the protonic conductivity, which has a significant impact on the performance of a PEMWE. In order to ensure the gas tightness of the PEMWE and increase the thermal and electrical connectivity between the different layers, the entire electrolyzer is compressed. Whether and in which way the swelling of the CCM is influenced by applying pressure or influences the surrounding layers is investigated in this study using a special compression device and X-ray computer tomography (CT). CT scans were carried out and the resulting cross-sectional images analyzed. Five different compression pressures between 0.36 and 1.63 MPa were applied for the dry (28 °C, atmospheric humidity) and wet (28 °C, surrounded by liquid water) states. The thickness change of the CCM and adjacent porous transport layers (PTL) was then measured. Due to the compression pressure, the thickness of the CCM decreased by 5%. For lower pressures, the carbon paper PTL compensates more of the swelling than the titanium felt PTL. For higher pressures, the ratio is inverse.

https://doi.org/10.1016/j.jpowsour.2023.233242
Received 29 March 2023; Received in revised form 5 May 2023; Accepted 21 May 2023
Available online 6 June 2023

1. Introduction

As the proton conductivity of the catalyst coated membrane (CCM) of a polymer electrolyte membrane (PEM) water electrolyzer (PEMWE) depends on the membrane's water content [1], a fully saturated membrane should be ensured to have the highest protonic conductivity. When a membrane takes up water, the thickness of the Nafion® membranes 112, 115, 117 changes in the range of 9 to 43.2% [2,3]. In addition to the type of membrane, the thickness change also depends on the water temperature [1,2,4–8]. At 100 °C, Nafion® 117 swells by 18.9% and at 170 °C by 43.2% [2]. For the catalyst coated Nafion® membrane NRE212 that was also used in this study, Folgado et al. [9] and Folgado et al. [10] measured an unconstrained thickness increase of about 30% from a dry thickness of 51 μm to a humidified (23 °C) one of about 66 μm. The expansion of the membrane and the CCM, respectively, results in a swelling strain [11–13]. Satterfield et al. [11] measured a swelling pressure of 0.55 MPa at a temperature of 80 °C for a Nafion® 115 membrane. For that, they placed the membrane between two porous plates, evacuated the chamber, and introduced humidified air (0–100%) into it. In contrast to Satterfield et al. [11], Escoubes et al. [12] and Borgardt [13] measured the swelling pressure after the membranes were flooded with liquid water. Borgardt [13] clamped the membrane between a solid and porous plate and flooded the compression cell. A swelling pressure of 30 MPa was measured. Escoubes et al. [12] saw a pressure of 1–1.3 MPa for unconstrained conditions. When the membrane is constrained from expanding in-plane, the swelling pressure increases to 50 MPa. This swelling pressure is opposed to the pressure required for gas tightness and the electrical and thermal connection of the different layers in an electrolyzer cell. From the literature, it is known that the performance of the electrolyzer cells increase with higher clamping pressures [14–16]. Frensch et al. [16] investigated the influence of compression pressure on the performance of an electrolyzer. The authors observed an increase in the performance with increasing clamping pressure up to 3.75 MPa, which was a local optimum. Similar to Frensch et al. [16], Al Shakhshir et al. [14] and Borgardt et al. [15] also studied the effect of clamping pressure on the cell performance of a PEMWE. Both noted an increase in the cell performance with increasing clamping pressure, but only Borgardt et al. [15] recorded a global optimum at 2.55 MPa. Depending on the specific cell design, Borgardt et al. [15] outlined a cell design featuring an expanded mesh without any PTLs (design a in [15]) and for a cell design without an expanded mesh, but with a sintered PTL and a carbon paper (design c in [15]), whereby the ohmic resistance did not change at pressures higher than 3 MPa. For a slightly different configuration in comparison to design a (with a carbon felt between the CCM and the expanded mesh on one side; design b in [15]), Borgardt et al. [15] found that the ohmic resistance increases at clamping pressures higher than 3 MPa. For design b, the authors could only explain the increase by the decrease in the protonic conductivity. Compared to our configuration as described below in the experimental setup, design c fits best as the bipolar plate without flow field and the expanded mesh can both be treated as incompressible. In this study, we conduct an ex-situ experiment using X-ray tomography and the compression device developed by Hoppe et al. [17]. We intend to determine the impact of cell compression on the thickness of a catalyst coated Nafion® 212 membrane in an electrolyzer configuration. Furthermore, we analyze the thickness change of the CCM due to swelling and the impact on the thickness change of the surrounding PTLs. In addition, the effect of compression and swelling on the porosity is investigated.

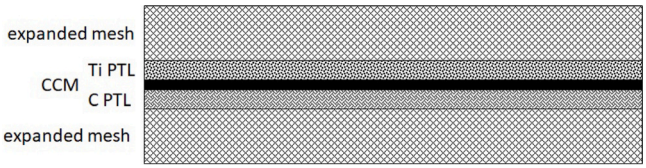

Fig. 1. Sketch of the current sample/cell design.

2. Experimental setup

In order to represent the conditions in a real PEM water electrolyzer as realistically as possible, the same components as in the 400 kW stack set up by Janßen et al. [18] were used. Beginning from the top, the investigated sample consists of (Fig. 1):

- Expanded metal sheet (2640 μm, titanium)
- Bekaert 2GDL10-0,35 (355 μm, anode, titanium)
- CCM (50 μm, Nafion® 212 membrane)
- Toray TGP-H-120 (345 μm, cathode, carbon)
- Expanded metal sheet (2640 μm, titanium)

with the initial thickness of each layer in brackets (see Fig. 3). With the exception of the CCM, which was made in-house [19], the other components are commercially-available. To gain a clearer picture of the expanded metal sheet, a CT scan is shown in Fig. 2. The sheet consists of three different layers with different mesh sizes to gain a homogeneous water distribution. Fig. 2(b) shows the cross-section of the finest mesh which is in contact with the PTLs. As we have no additional flow field plate with a land and channel structure, the white and black area are the land and channel, respectively.

In the following we will use the term PTL for both, the titanium (Ti-PTL) and carbon (C-PTL) transport layer. In contrast to the fuel cell, in an electrolyzer diffusion is not the dominating effect for gas transportation. Therefore, we are not using the term gas diffusion layer.

To compress the above-mentioned components and investigate the impact of compression on the CCM swelling, a special compression device was used [17]. The sample was placed between the ceramic block and the pedestal. By utilizing the screw, the components can be compressed. The compression device, including the sample, is then placed in the computer tomograph (CT) Xradia Versa 410 from Carl Zeiss AG. In contrast to the scanning electron microscope, the CT scan can provide a 3D model (tomogram) of the sample, rather than a single surface image. Thereby, the inside of the compressed sample can be analyzed. To obtain a tomogram, the sample was placed between the X-ray source and detector of the CT. The sample was rotated by 360° and a defined number of projections were taken and the tomogram was reconstructed. The parameter list for the CT settings is shown in Table 1.

Using the tomogram, 2D slices (see Fig. 3) can be derived to analyze the inner structure of the above-mentioned sample stack and in particular the thickness change of the CCM and the surrounding layers due to compression and membrane swelling, including the change in porosity of the porous layers.

2.1. Experimental procedure

To investigate the influence of the compression on the layer thicknesses and swelling of the CCM, the procedure shown in Fig. 4 was applied. First, the different layers were stacked in order to prepare the

* Corresponding author.
E-mail address: e.hoppe@fz-juelich.de (E. Hoppe).

Table 1
Parameter CT.

Parameter	Value
Acceleration voltage	100 kV
Power	7 W
Exposure time	30 s
Distance source-sample	62 mm
Distance detector-sample	62 mm
Number of projections	2001
Rotation angle	360°
Optical magnification	4 X
Binning	2
Filter	HE6
Voxel size	3.36 µm

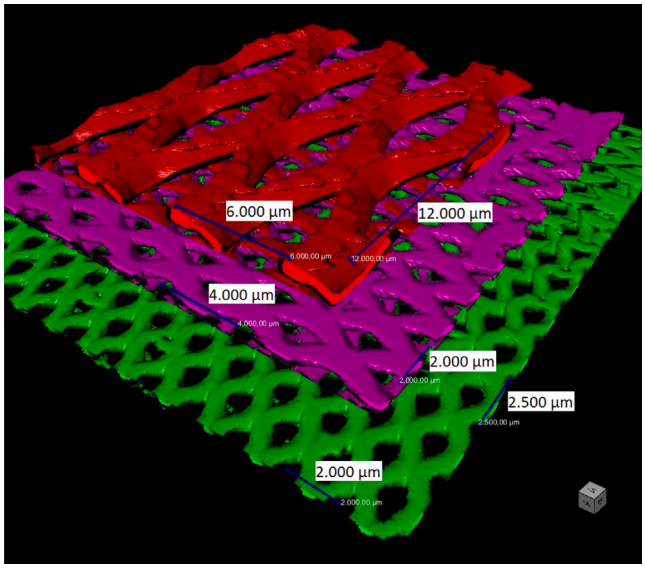

(a) 3D view.

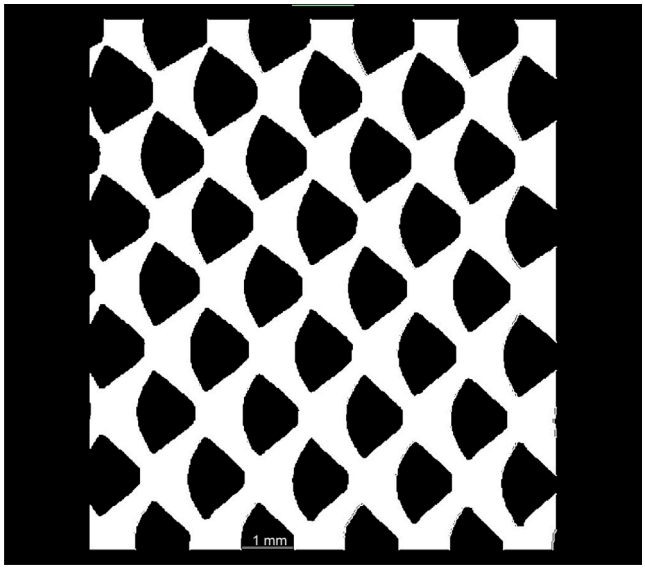

(b) Cross-section of the expanded metal sheet showing the lands (white area) and channels (black area).

Fig. 2. CT scan of the expanded metal sheet used.

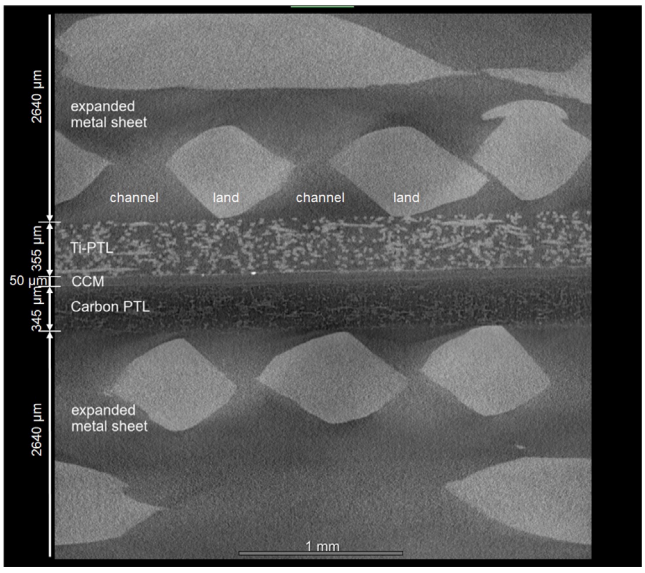

Fig. 3. 2D slice of the compressed sandwich, derived from a tomogram.

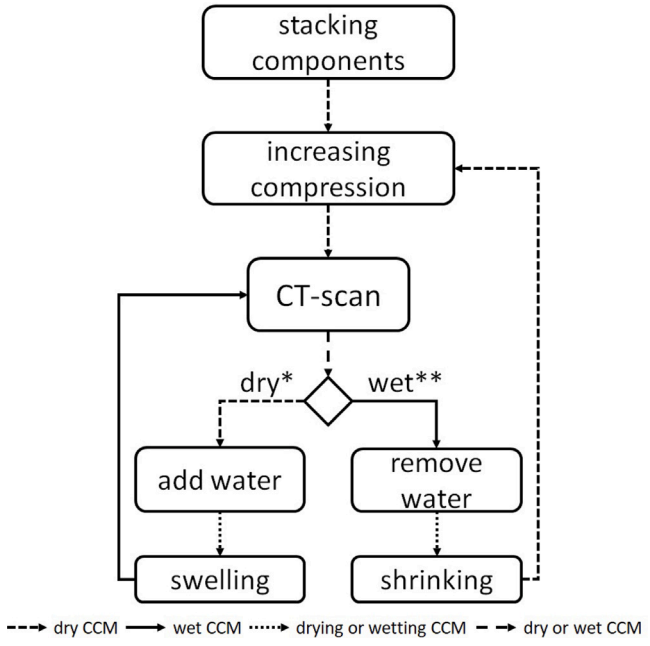

Fig. 4. Procedure applied to investigate the influence of compression on layer thickness and CCM swelling; *28 °C and atmospheric humidity; **28 °C and liquid water.

test sample. Then, a first compression pressure was applied and a CT scan performed. Then, depending on the state of the CCM (dry* or wet**), either water was added so it swelled or water removed so it shrank. If the CCM was wet, a CT scan with the same compression pressure as the dry sate was performed. If the CCM was dry, the compression pressure was increased and a CT scan performed. This process was repeated for five compression pressures in total, meaning that five CT scans of the dry state and five of the wet state were performed. At the end, a pair of scans (dry and wet CCM) for each compression pressure was achieved.

In this study, the dry state refers to room temperature (28 °C in the computer tomograph chamber) and ambient humidity. The wet state is defined as the CCM is completely surrounded by liquid water at 28 °C.

Before carrying out the actual measurement, a pre-series (same conditions as the actual measurement) was performed using a force

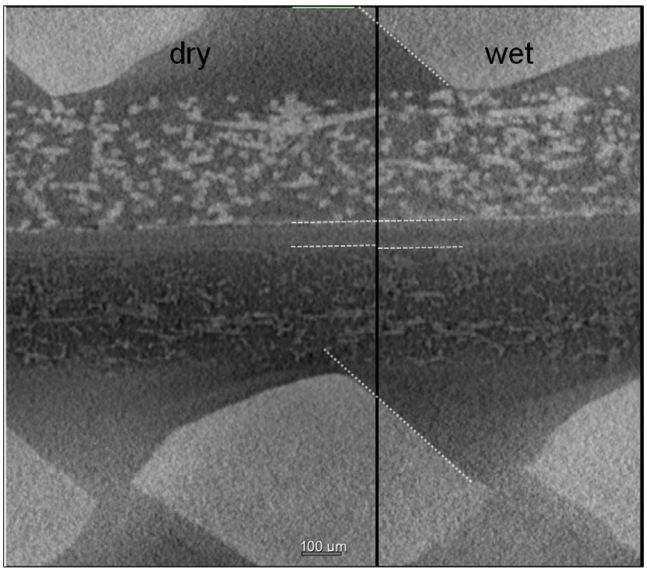

Fig. 5. Comparison of the dry (left) and wet (right) states of the CCM under compression.

sensor between the screw and sample sandwich. Analyzing the 2D slices of the different compression rates, the thicknesses of the stacked sample could be related to the different force values measured with the force sensor. This pre-series measurement was employed to derive a relationship between the force, the compression pressure, and thickness of the sample, respectively. During the actual measurement series, the thicknesses of the sample sandwich at the different compression rates was measured. Using the derived relationship from the pre-series, the compression pressure was calculated.

The pre-series showed that the force sensor acted like a suspension element when the CCM swelled. This led to different distances of the expanded metal sheets for the dry an wet state. To keep the distance constant, the force sensor was omitted in the actual measurement series. Furthermore, the pre-series also showed that the water uptake of the CCM in liquid water lasts less than 100 s as was shown by Zawodzinski et al. [1] for a Nafion® 117 membrane. Therefore, the CT scans could be performed directly and in succession.

3. Results and discussion

Compression pressures ranging from 0.36 to 1.63 MPa were applied and CT scans according to the scheme in Fig. 4 for the dry and wet stats carried out. Fig. 5 shows two 2D cross-sections of a compression pressure of 0.36 MPa. On the left side the dry CCM can be seen and on the right, the wet (flooded). A first look at the two CT scans (Fig. 5) and a deeper analysis of all compression rates showed that, for a constant compression pressure, the distance between the two expanded metal sheets of the anode and cathode sides did not change due to the CCM swelling. It can be concluded from this that any change in thickness due to CCM swelling affects only the two PTLs and the CCM itself. Whether and to what extent PTL thicknesses change due to CCM swelling will be discussed later. First, it will be discussed whether or not the CCM swelling is constrained by compression.

3.1. Membrane swelling

As the protonic conductivity of the membrane of a CCM depends strongly on the latter's water content [1] and the thickness of the CCM corresponds to the water content [2,3], by implication the CCM thickness is an indicator of the protonic conductivity. As a certain pressure is needed for the electrical and thermal conductivity of the different layers, it is important to know how the compression pressure affects the CCM swelling. Therefore, the dry and wet thicknesses for different compression pressures and two different locations in the cell, shown in Fig. 6, were measured. For each compression pressure, the average thicknesses at ten different points were calculated. The dry thickness in the land region (Fig. 6(a)) ranged between 47.9 ± 1.1 µm and 50.1 ± 0.9 µm and the wet thickness from 62.4 ± 2.2 µm to 65.8 ± 0.9 µm. The dry and wet thicknesses, where the channels of the anode and cathode sides face each other, are in the same range as for the land-facing region. At first, this indicates that the CCM swelling is independent from the position within the electrolyzer cell.

As the wet thickness of the CCM is higher than the dry thickness for the entire compression range for both the land and channel regions, this observation suggests that the water uptake of the CCM is not fully inhibited at high pressures. For both the dry and wet thickness, no clear tendency regarding a constraint in water uptake can be observed. In average, over all compression pressures, the dry thickness is about 49.4 ± 1.0 µm and the wet about 63.9 ± 1.4 µm - a thickness increase of 30% (land region). For the channel region, the thickness increases by 25%. For both, the deviation lies under the resolution of 3.36 µm of the CT scans. The dry and wet thicknesses, even for high compression pressures, are in very good agreement with Folgado et al. [9] and Folgado et al. [10], who measured the unconstrained swelling of a Nafion® NRE212 membrane at room temperature. Within the scope of accuracy of the CT scans, this indicates that even when applying pressure, the swelling of the CCM in the electrolyzer configuration is unconstrained. As the swelling is unconstrained, the water uptake of the CCM is not affected by the compression, which leads to the conclusion that the protonic conductivity remains constant over the investigated pressure range. Therefore, for this configuration, a potential decrease in electrolyzer performance with increasing pressure cannot be assigned to the clamping pressure.

Leaving accuracy aside, the dry and wet thickness of the CCM in the land region decreases slightly (about 4 and 5% for the dry and wet states, respectively). Although the absolute thickness decreases for the dry and wet CCM, the thickness from the dry to wet states does not change much. For 0.36 and 1.29 MPa, the thickness increases by 16.0 and 16.7 µm, respectively. However, this only means that the amount of water absorbed remains approximately constant. The total water content in the CCM differs. The lower water uptake finally decreases not only the thickness but also the protonic conductivity of the CCM and so reduces the performance of the electrolyzer cell. This would then confirm the assumption of Borgardt et al. [15], that for design c, the increase in the ohmic resistance is attributed to the decreased protonic conductivity. Despite neglecting the accuracy, the thickness of the CCM in the channel region remains constant over the investigated pressure range. This can be simply explained by the fact that the force is mostly transmitted through the lands. For the entire active cell area of a PEMWE, this means that there are areas with a slightly decreased water content and so decreased protonic conductivity. To avoid this, the channel area should be increased to have a larger area, so that the protonic conductivity does not decrease. However, this would then worsen the pressure distribution over the active cell area, as well as the contact between the different layers of the cell and hence increase the ohmic resistance and in turn worsen the cell performance.

As the ohmic resistance is mostly measured for the entire cell, the spatial differences in the protonic conductivity cannot be resolved by the methods used in this experiment. As the ohmic resistance increases in some cases [15], this can be attributed to land regions. To validate the above-mentioned ex-situ findings, a spatially-resolved impedance spectroscopy analysis must be performed.

3.2. Thickness change of the PTLs

As a result of the thickness increase of the CCM and the constant distance between the expanded metal sheets at the same time, the PTL

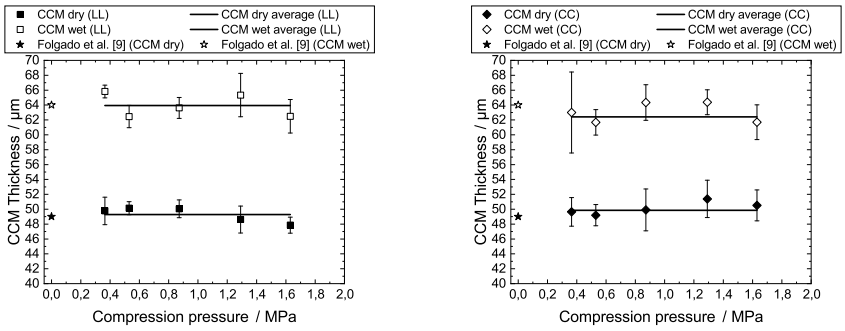

(a) Land facing land (b) Channel facing channel

Fig. 6. Dry (full rectangle) and wet (empty rectangle) thicknesses of the CCM for different compression pressures at different positions in the cell.

must decrease in thickness. Fig. 7 shows the swelling and compression of the three different layers for the five investigated pressure levels for the land (Fig. 7(a)) and channel region (Fig. 7(b)). It should be mentioned that for the CCM, the thickness change is positive (increasing thickness) and for the PTLs, negative (decreasing thickness). For better comparability, both thickness changes are plotted in the same direction. Furthermore, the thicknesses of the CCM and both PTLs at the different compression pressures divided by their initial thicknesses (normalized thickness) are shown in Fig. 7.

At lower pressures, the C-PTL compensates about 75% (e.g. 11.7 µm of 16 µm at 0.36 MPa) of the CCM swelling and is compressed by 10–30% at pressures of 0.36–0.87 MPa, respectively. Comparing the clamping pressure of less than 1 MPa with the swelling pressure of 30 MPa [12] at a temperature of 20 °C, it is not surprising that the PTLs are compressed due to the swelling as the distance of the expanded metal sheets remains constant. At higher compression pressures, the C-PTL is compressed by more than 50%, but only compensates 2 µm of the 15 µm swelling, which is 13% of the CCM swelling. At the same time the Ti-PTL is only compressed by 13% but compensates 87% of the CCM swelling. This could be explained by the different mechanical behaviors of the Ti-PTL and C-PTL. For compression pressures up to 1.5 MPa, the C-PTL is compressed twice as much as the Ti-PTL, which explains the higher compensation rate of the C-PTL at lower compression pressures [20–23]. For higher strains, no data is available in the literature. However, we would assume that the thickness change of the C-PTL will end in a saturation. That means a high pressure is needed to further compress the PTL. This would explain the changing compensation ratio of the PTLs. Considering a temperature of about 80 °C during electrolyzer operation and an enhanced water uptake of the membrane [1,2,4–8], the swelling pressure and so the deformation of the PTLs could also be increased further. This is only true to a certain point, as with decreasing PTL thickness the needed compression pressure drastically increases. With a porosity of approximately 70%, the C-PTL can theoretically only be compressed to a normalized thickness of 30% (assuming no in-plane expansion). At the highest compression, the C-PTL is already compressed to a normalized thickness of 47%. To further deform the C-PTL, a significantly higher pressure (> 10 MPa/100 bar) is needed. Therefore, for very high compression rates, either the Ti-PTL would be compressed more or the swelling of the CCM would be constrained. As the best performance of an electrolyzer is already reached at low compression pressures, this case will never arise in a normal electrolyzer stack. The effect of a differential pressure of, for example 30 bar (3 MPa), as it occurs in some electrolyzer stacks, cannot be investigated with the used compression device as it is open to atmosphere. In contrast to the land facing land region, at the channel facing channel region (see Fig. 7(b)), the PTLs do not compensate the entire swelling of the CCM. This is due to the free space of the channel, where both PTLs can intrude in. Nevertheless, a thickness decrease of the PTLs can be seen. With increasing clamping pressure the thickness decrease due to CCM swelling becomes smaller. This indicates that the intrusion of the PTLs into the channel increases. Contrary to the first region, the normalized thickness especially of the C-PTL does not decrease that much (82% at 1.63 MPa).

3.3. Porosity

The change in thickness of the PTLs is also accompanied by a change in porosity. In this specific case, there are two factors that influence the change in thickness and porosity, namely the compression pressure due to clamping (outer force- on the one hand), and the swelling pressure (inner force) on the other hand.

In the region of the PTLs, the CT scan does not show a bimodal histogram, so it cannot be binarized by using analytical methods to determine the porosity. The Dragonfly software, Version 2022.2 for Windows, has a deep learning tool that can be trained to distinguish between fibers and surrounding fluid (air for the dry state and water for wet one). Fig. 8 shows the porosity of the two PTLs depending on the compression pressure. As expected, the porosity for both PTLs decreases with increasing pressure. The porosity of the C-PTL decreases quite linearly from 65.9% at 0.36 MPa to 58.7% at 1.63 MPa. As can be seen in Fig. 7, Toray compensated for most of the thickness increase of the CCM, and therefore it is not surprising that the decrease in the porosity from 65.9% (dry) to 63.9% (wet) at 0.36 MPa is fairly high. With increasing compression, this difference decreases. The same holds true for the Ti-PTL. The decrease of porosity from the dry to wet states is in the range of 1 to 2 percentage points. At a compression pressure of 0.87 MPa, it seems that the porosity increases due to membrane swelling and decreasing thickness. This can presumably be attributed to the model for binarization, as the intensity of the fibers and air or water may differ little and the model predicts the fibers and fluid inaccurately. Furthermore, it is surprising that the porosity of the Ti-PTL decreases in the same range as that of the C-PTL, although the thickness of Ti-PTL decreases by only 13% in total, whereas the C-PTL decreases by 53% and exhibits the same porosity progression. Nevertheless, the porosity does not decrease to a value that could be critical for mass transport, as there are PTLs with lower porosities (35–40% in comparison to 58%) that do not show significant mass transport resistance nor significant influence on cell performance [24].

4. Conclusions

As an electrolyzer cell and stack consists of many different layers and components, it is, on the one hand, important to analyze and improve each component separately, but on the other, all components, especially with respect to the mechanics, interact with one another. Therefore, it is just as important to analyze the entire assembly. Otherwise, interactions between the components cannot be identified. In

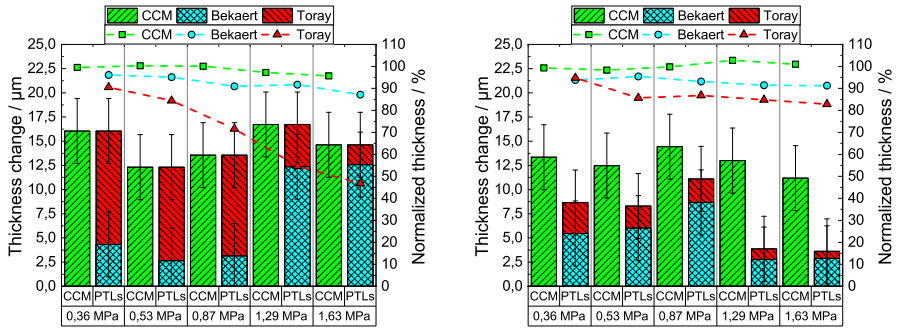

(a) land facing land (b) channel facing channel

Fig. 7. Left axis: Thickness change of the CCM and PTLs due to CCM swelling. The CCM increases in thickness, whereas the PTLs decrease in thickness. Right axis: Normalized dry thickness.

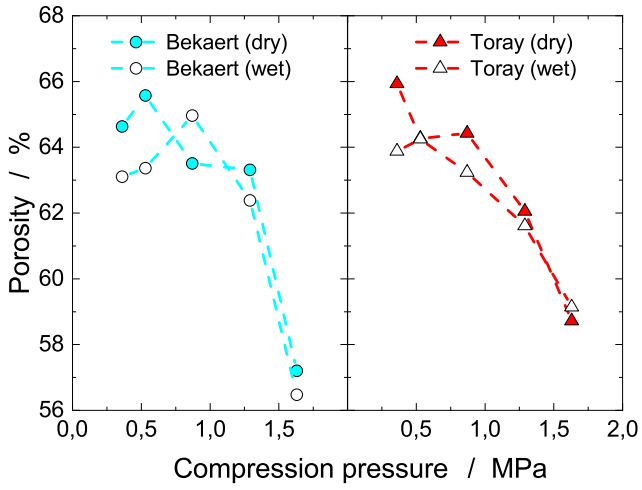

Fig. 8. PTL porosity for the dry and wet state at different compression pressures.

this study, we took a closer look at the interaction between the CCM and porous layers. When looking at the swelling of the Nafion NRE212 membrane in a PEM water electrolyzer, a general statement regarding the constraint of the swelling could not be made. A distinction between two areas must be made. In the first, the land regions of the anode and cathode side face each other and in the second, the channels of the flow field do. The thickness decrease in the first area is about 5% for both the dry and the wet thicknesses. In the second area, no change in thickness due to increasing compression (clamping) pressure can be noticed. Therefore, a change (increase) in the ohmic resistance, which is dominated by the protonic conductivity of the membrane, above a certain pressure can be attributed to the first area, where the membrane takes up less water and so reduces the protonic conductivity. The swelling of the CCM causes a decrease in the thickness of the surrounding PTLs in the order of 5–12 µm which leads to a porosity decrease of only 1percentage point. Consequently, an influence on the mass transport and a potential increase in a mass transport limitation due to the swelling cannot be observed.

CRediT authorship contribution statement

Eugen Hoppe: Writing – original draft, Methodology, Visualization, Investigation, Conceptualization, Formal analysis. **Sebastian Holtwerth:** Investigation, Resources, Conceptualization. **Martin Müller:** Writing – review & editing, Conceptualization. **Werner Lehnert:** Supervision, Writing – review & editing, Conceptualization, Project administration.

Declaration of competing interest

The authors declare that they have no known competing financial interests or personal relationships that could have appeared to influence the work reported in this paper.

Data availability

Data will be made available on request.

Acknowledgments

funded by the Deutsche Forschungsgemeinschaft (DFG, German Research Foundation) – 491111487

References

[1] T.A. Zawodzinski, C. Derouin, S. Radzinski, R.J. Sherman, V.T. Smith, T.E. Springer, S. Gottesfeld, Water-uptake by and transport through Nafion(R) 117 membranes, J. Electrochem. Soc. 140 (4) (1993) 1041–1047, http://dx.doi.org/10.1149/1.2056194.

[2] T. Sakai, H. Takenaka, N. Wakabayashi, Y. Kawami, E. Torikai, Gas permeation properties of solid polymer electrolyte (spe) membranes, J. Electrochem. Soc. 132 (6) (1985) 1328–1332, http://dx.doi.org/10.1149/1.2114111.

[3] F.N. Büchi, G.G. Scherer, Investigation of the transversal water profile in nafion membranes in polymer electrolyte fuel cells, J. Electrochem. Soc. 148 (3) (2001) http://dx.doi.org/10.1149/1.1345868.

[4] R.W. Kopitzke, C.A. Linkous, H.R. Anderson, G.L. Nelson, Conductivity and water uptake of aromatic-based proton exchange membrane electrolytes, J. Electrochem. Soc. 147 (5) (2000) 1677–1681, http://dx.doi.org/10.1149/1.1393417.

[5] J. Benziger, A. Bocarsly, M.J. Cheah, P. Majsztrik, B. Satterfield, Q. Zhao, Mechanical and transport properties of nafion: Effects of temperature and water activity, in: Fuel Cells and Hydrogen Storage, in: Structure and Bonding, 2011, pp. 85–113, http://dx.doi.org/10.1007/430_2011_41.

[6] A. Parthasarathy, S. Srinivasan, A.J. Appleby, C.R. Martin, Temperature dependence of the electrode kinetics of oxygen reduction at the platinum/Nafion® interface—A microelectrode investigation, J. Electrochem. Soc. 139 (9) (2019) 2530–2537, http://dx.doi.org/10.1149/1.2221258.

[7] J.T. Hinatsu, M. Mizuhata, H. Takenaka, Water uptake of perfluorosulfonic acid membranes from liquid water and water vapor, J. Electrochem. Soc. 141 (6) (2019) 1493–1498, http://dx.doi.org/10.1149/1.2054951.

[8] M. Yoshitake, M. Tamura, N. Yoshida, T. Ishisaki, Studies of perfluorinated ion exchange membranes for polymer electrolyte fuel cells, Denki Kagaku Oyobi Kogyo Butsuri Kagaku 64 (6) (1996) 727–736, http://dx.doi.org/10.5796/kogyobutsurikagaku.64.727.

[9] M.A. Folgado, P. Ferreira-Aparicio, A.M. Chaparro, Study of the constrained expansion of nafion within the hardware of a PEMFC, ECS Trans. 64 (3) (2014) 729–738, http://dx.doi.org/10.1149/06403.0729ecst.

[10] M.A. Folgado, P. Ferreira-Aparicio, A.M. Chaparro, An optical and single cell study of the assembly of a PEMFC with dry and expanded Nafion, Int. J. Hydrogen Energy 41 (1) (2016) 505–515, http://dx.doi.org/10.1016/j.ijhydene.2015.10.120.

[11] M.B. Satterfield, P.W. Majsztrik, H. Ota, J.B. Benziger, A.B. Bocarsly, Mechanical properties of Nafion and titania/Nafion composite membranes for polymer electrolyte membrane fuel cells, J. Polym. Sci. B 44 (16) (2006) 2327–2345, http://dx.doi.org/10.1002/polb.20857.

[12] M. Escoubes, M. Pineri, E. Robens, Application of coupled thermal-analysis techniques to thermodynamic studies of water interactions with a compressible ionic polymer matrix, Thermochim. Acta 82 (1) (1984) 149–160, http://dx.doi.org/10.1016/0040-6031(84)87283-4.

[13] E. Borgardt, Mechanical Properties of Catalyst Coated Membranes for Polymer Electrolyte Membrane Electrolysis (Dissertation), 2020, http://dx.doi.org/10.18154/RWTH-2021-04026.

[14] S. Al Shakhshir, X. Cui, S. Frensch, S.K. Kær, In-situ experimental characterization of the clamping pressure effects on low temperature polymer electrolyte membrane electrolysis, Int. J. Hydrogen Energy 42 (34) (2017) 21597–21606, http://dx.doi.org/10.1016/j.ijhydene.2017.07.059.

[15] E. Borgardt, L. Giesenberg, M. Reska, M. Müller, K. Wippermann, M. Langemann, W. Lehnert, D. Stolten, Impact of clamping pressure and stress relaxation on the performance of different polymer electrolyte membrane water electrolysis cell designs, Int. J. Hydrogen Energy 44 (42) (2019) 23556–23567, http://dx.doi.org/10.1016/j.ijhydene.2019.07.075.

[16] S.H. Frensch, A.C. Olesen, S.S. Araya, S.K. Kær, Model-supported characterization of a PEM water electrolysis cell for the effect of compression, Electrochim. Acta 263 (2018) 228–236, http://dx.doi.org/10.1016/j.electacta.2018.01.040.

[17] E. Hoppe, H. Janßen, M. Müller, W. Lehnert, The impact of flow field plate misalignment on the gas diffusion layer intrusion and performance of a high-temperature polymer electrolyte fuel cell, J. Power Sources 501 (2021) http://dx.doi.org/10.1016/j.jpowsour.2021.230036.

[18] H. Janßen, S. Holtwerth, W. Zwaygardt, A. Stähler, W. Behr, D. Federmann, M. Carmo, W. Lehnert, M. Müller, Novel development approach for optimized bipolar plate units in polymer electrolyte membrane electrolyzers, Int. J. Hydrogen Energy (2023) submitted for publication.

[19] M. Stähler, A. Stähler, F. Scheepers, M. Carmo, D. Stolten, A completely slot die coated membrane electrode assembly, Int. J. Hydrogen Energy 44 (14) (2019) 7053–7058, http://dx.doi.org/10.1016/j.ijhydene.2019.02.016.

[20] N. Khajeh-Hosseini-Dalasm, T. Sasabe, T. Tokumasu, U. Pasaogullari, Effects of polytetrafluoroethylene treatment and compression on gas diffusion layer microstructure using high-resolution X-ray computed tomography, J. Power Sources 266 (2014) 213–221, http://dx.doi.org/10.1016/j.jpowsour.2014.05.004.

[21] E. Sadeghi, N. Djilali, M. Bahrami, Effective thermal conductivity and thermal contact resistance of gas diffusion layers in proton exchange membrane fuel cells. Part 1: Effect of compressive load, J. Power Sources 196 (1) (2011) 246–254, http://dx.doi.org/10.1016/j.jpowsour.2010.06.039.

[22] A. Radhakrishnan, Z. Lu, S.G. Kandlikar, Effective thermal conductivity of gas diffusion layers used in PEMFC: Measured with guarded-hot-plate method and predicted by a fractal model, ECS Trans. 33 (1) (2010) 1163–1176, http://dx.doi.org/10.1149/1.3484610.

[23] N.B. SA, Technical data sheet, 2021, URL: https://www.bekaert.com/-/media/Files/Download-Files/BFT/Porous-transpart-layers.pdf.

[24] S.A. Grigoriev, P. Millet, S.A. Volobuev, V.N. Fateev, Optimization of porous current collectors for PEM water electrolysers, Int. J. Hydrogen Energy 34 (11) (2009) 4968–4973, http://dx.doi.org/10.1016/j.ijhydene.2008.11.056.